GLOBAL SURFACE ALBEDO FROM CERES/TERRA SURFACE AND ATMOSPHERIC RADIATION BUDGET (SARB) DATA PRODUCT

David Rutan[1] and Thomas P. Charlock[2], Fred Rose[1], Seiji Kato[3],
Scott Zentz[4], and Lisa Coleman[4]

[1]Analytical Services and Materials Inc., Hampton, VA
[2]NASA Langley Research Center, Atmospheric Sciences Competency, Hampton, VA.
[3]Hampton University, Hampton, VA.
[4]Science Applications International Corp. Hampton, VA.

Introduction

Within the Clouds and the Earth's Radiant Energy System (CERES) science team (Wielicki et al. 1996), the Surface and Atmospheric Radiation Budget (SARB) group is tasked with calculating vertical profiles of heating rates, globally, and continuously, beneath CERES footprint observations of Top of Atmosphere (TOA) fluxes. This is accomplished using a fast radiative transfer code originally developed by Qiang Fu and Kuo-Nan Liou (Fu and Liou, 1993) and subsequently highly modified by the SARB team. Details on the code and its inputs can be found in Kato et al. (2005) and Rose and Charlock (2002). The radiative transfer (SARB) subsystem currently has archived flux profiles at footprint (~20km) and grid box spatial scale. This paper details the release of albedo maps based on 1-degree gridded broadband surface shortwave flux calculations.

SARB Data Products

The first archived data product from the SARB group is the "Clouds and Radiative Swath" or CRS. This product is a combination of the CERES Single Satellite Flux (SSF) data product and the model inputs and radiation transfer calculations that characterize atmospheric conditions (surface properties, atmospheric profiles, cloud properties, and aerosol properties) below a CERES footprint (~20km at nadir.) Though the radiation transfer code is run at a higher vertical resolution, radiative fluxes are archived at five levels, TOA, 70hPa, 200hPa, 500hPa, and the Surface. The second CERES/SARB archived data product is a spatially averaged version of CRS data known as the Fixed Swath Width (FSW). This product collects all variables from the CRS and spatially averages them into 1-degree equal angle grid boxes. Because of the large data volume, FSW is released in groups of zonal bands for a month of data. Again, because of large data volume the SARB group has combined the FSW latitudinal data files, averaged the data over time, and produced clear and cloudy sky, monthly mean surface albedo maps from model output surface fluxes. It is these surface albedo maps, which are based heavily on broadband CERES observations under clear conditions that are presented in this monograph.

SARB Broadband Surface Albedo

The Langley-Fu & Liou radiation transfer code currently models 18 spectral intervals

Corresponding Author:
David Rutan
1 Enterprise Pkwy Suite 300
Analytical Services and Materials Inc,
Hampton, VA, 23666 (d.a.rutan@larc.nasa.gov)

in the shortwave (SW) spectrum. Hence for each daytime run of the code, both a scene dependent spectral shape and an initial estimate of broadband surface albedo are required. To determine these values the SARB algorithm uses a logic sequence based on scene type determined by MODIS imager pixels collocated within the larger CERES footprint and a fixed 1/6 degree equal angle resolution surface scene type from International Geosphere Biosphere Programme (IGBP). After scene type and cloud fraction (Minnis et al. 1995) are determined the algorithm chooses between several look-up tables based on radiative transfer models to estimate an initial broadband albedo. (Relative spectral albedo shape, not absolute magnitude, are tied to surface scene type over the land and do not vary with season except for snow and ice.) All water scenes utilize a look-up table based on the Coupled Ocean Atmosphere Radiation Transfer (COART) (Jin et al, 2004). This model supplies a spectral ocean albedo under all and clear sky conditions as a function of solar zenith angle, wind speed, and the optical depth of aerosol/cloud.

For land, determining surface albedo is more complex. If the MODIS imager determines the footprint to be cloud free then broadband surface albedo is determined from a look-up table based on the Langley Fu & Liou model. This table is a function sun angle, precipitable water, aerosol optical depth (from MODIS on board Terra Kaufman et al. 1997, and Collins et al, 2001), ozone, surface height, surface spectral shape, and aerosol type. This same model is used as a "pre-processor" where all clear sky footprints for a month are examined in advance of running the full radiation transfer code. For this pre-processed month, minimum clear sky albedos are saved on a 1/6 degree equal angle resolution grid. If a grid box is cloudy for the entire month a

historical value is retained or it is based solely on assumed surface vegetation type. This pre-processed "history" map is then used for cloudy sky footprints over land. The final piece is the determination of albedo over snow and ice. For clear sky footprints snow and ice albedo are determined from a lookup table again based on the COART model. For thin cloud cases the Langley Fu & Liou has been parameterized and for thick clouds over snow/ice albedo is based on spectral shapes developed from ground observations. The importance of describing the algorithm used to estimate an initial albedo is that the subsequent albedo, determined from surface fluxes from the radiation transfer code, is highly dependent on this initial estimate, particularly for clear skies.
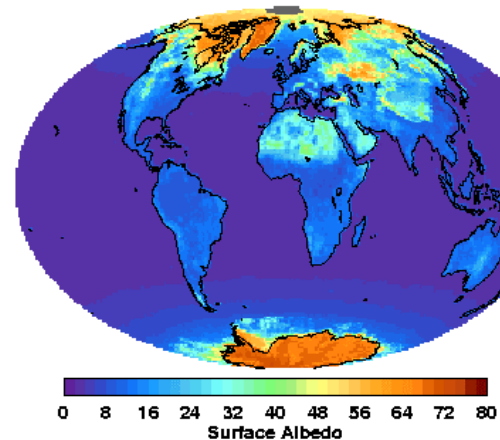

Figure 1. Clear sky monthly mean surface albedo for March 2000 from CERES FSW data product.

Global Surface Albedo Maps

Once instantaneous footprint (CRS) results are gridded to 1-degree maps in the FSW data product, gridded *monthly mean* flux profile products can be developed. A number of monthly mean variables can be found at:
http://asd-www.larc.nasa.gov/sarb/fsw_plots.html
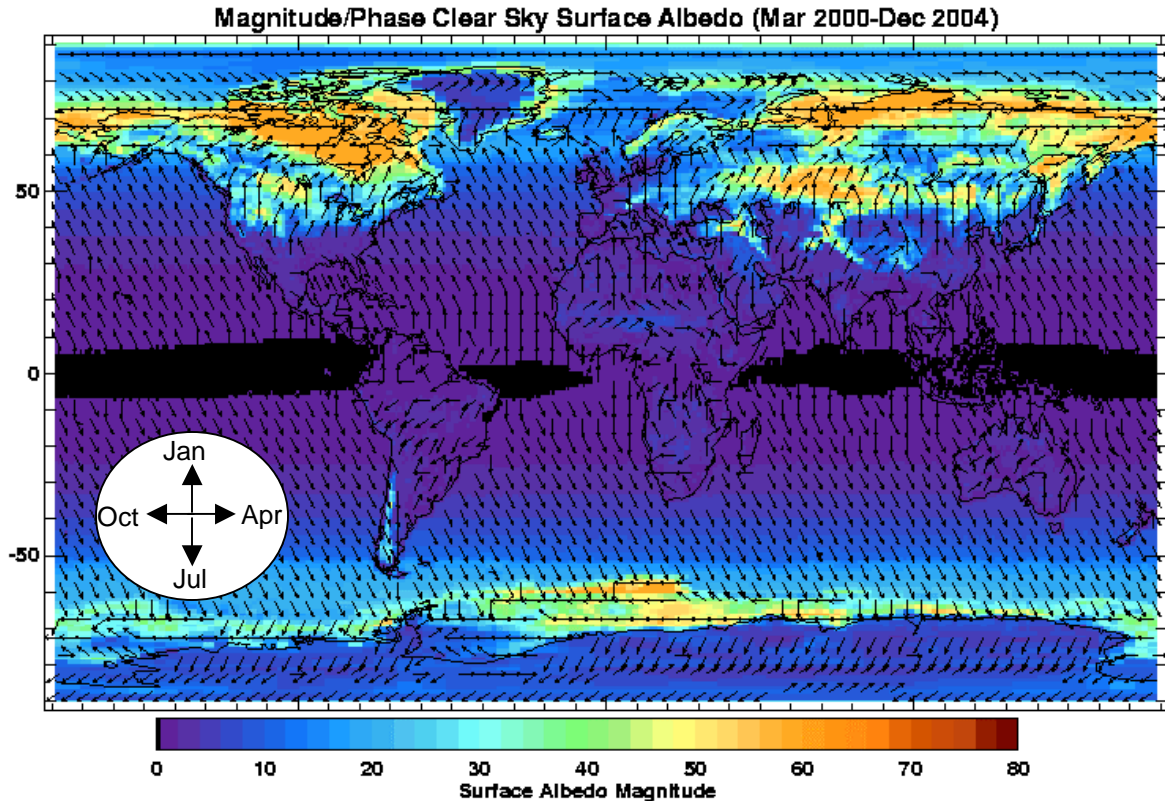For our purpose upward and downward surface flux results are ratioed to determine

Figure 2. Magnitude and phase of largest changes in canonical monthly mean FSW albedo maps between Mar 2000 and Dec 2004.

clear and cloudy sky surface albedos for each month of available FSW data. Note that within each 1-degree box, footprints are collected at the time of CERES observation, which varies as a function of latitude over the month. The albedo in Figure 1, for March 2000, is then, the mean albedo for the mean solar zenith angle of all the observations within a given grid box. Though with an equator crossing time of ~10:30AM one could consider this a mostly morning albedo.

ASCII data files for each month have been made available via anonymous ftp and a web site developed to explain the maps and associated parameters. These data files include surface albedo, scene type, diurnal modeling coefficient and a snow/ice flag for each 1-degree grid box. In SARB processing we use the simple 1-parameter diurnal

model developed by Briegleb et al. (1986) based on Dickinson, 1983. Included in each file is the "d" value as found in the following equation:

$$\alpha_1 = \alpha_1(1-d*\mu_0)/(1+2*\mu_1)$$

It is not recommend using this equation to model ocean surface albedo across the day. Instead the COART lookup table can be easily used and downloaded from: http://www-cave.larc.nasa.gov/jin/

To summarize the five years of albedo data, canonical monthly means were calculated and differenced, isolating the largest month-to-month changes. This can be represented as a "magnitude" (largest intra-month change) and "phase" (month largest change occurred.) This is plotted in Figure 2. The magnitude of the albedo changes is defined

by the color and arrows define the month when the largest change occurred with Jan pointing north and Jul pointing south. Over land the largest changes in surface albedo are associated with changes in snow cover during the winter season in higher latitudes. Other interesting effects can be found as well. For instance along the northern continental coastline and Antarctic coast the largest changes in albedo are coming as the sea ice recedes in May and October depending on the hemisphere. Also through the Sahel of Central Africa the largest change in albedo (though small relative to other changes) occurs during March for this 5-year period.
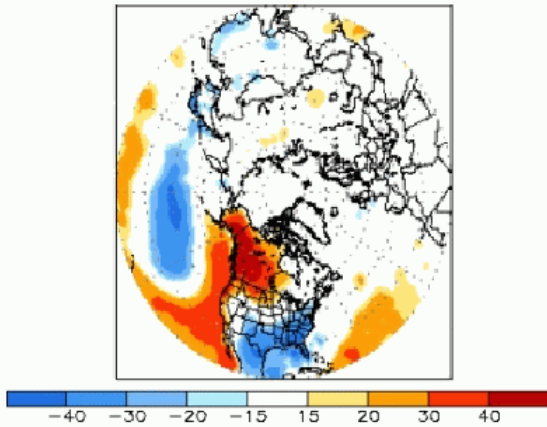

Figure 3. Spatial pattern showing PNA correlated to surface temperature anomalies for 3 months centered on January.
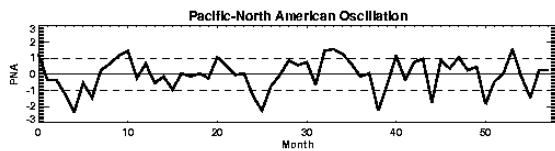

Figure 4. Temporal component the CPC's EOF analysis of PNA teleconnection.

FSW Albedo and the Pacific North American Oscillation

Given that the time series of albedo includes nearly 5 years of monthly means it is not unreasonable to attempt to tie this series with common climate indices. To that end,

as an example, the time series is compared to the well known Pacific North American Oscillation Index or PNA. The spatial pattern shown in figure 3 comes from the National Weather Service, Climate Prediction Center, EOF analysis of 500mb heights. The teleconnection pattern determined from the EOF analysis is then correlated to monthly surface temperature anomalies for the three months centered on January. Figure 4 shows the normalized time series associated with the PNA from the principal component analysis but only for the time coincident with the FSW albedo time series.
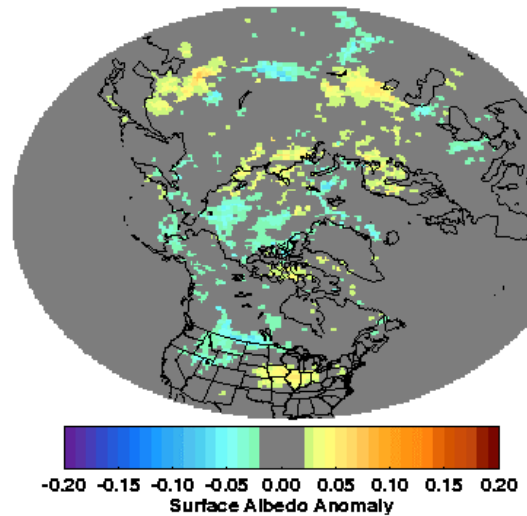

Figure 5. Composite map of FSW surface albedo to positive anomalies of the PNA seen in figure 4.

We associate the FSW surface albedo to the PNA by first calculating anomalies from the five-year mean for the albedo time series. Then we composite albedo anomaly maps associated with the positive and negative values in the PNA as found Figure 4. The resulting composite albedo for positive anomalies is shown in Figure 5. The positive anomaly of the PNA is generally associated with warmer/dryer weather across central US and western and south central Canada and cooler wetter weather across US Midwest and south east. These are clearly

seen as positive and negative anomalies in the spatial map in Figure 3. We find in the albedo composite associated with the positive PNA anomalies a lower/higher albedo in these locations correlated with the change in snowfall due to the PNA. Other interesting patterns are also found across southern Russia, the Caucuses and into China.

Data Distribution

The SARB/FSW global monthly mean albedo maps are available via anonymous ftp at:

http://www-cave.larc.nasa.gov/sfc_albedo

This web site describes the data files, explains the variables included in each file and has a plotting capability that allows quick looks at all 58 months of data.

Acknowledgements

CERES data is made available from NASA Langley's Atmospheric Sciences Data Center:
http://eosweb.larc.nasa.gov/

Plots of Pacific North American Oscillations and time series come from the National Weather Service, Climate Prediction Center (CPC):
http://www.cpc.ncep.noaa.gov/data/teledoc/pna.shtml

References

Briegleb, B.P., P. Minnis, V. Ramanathan, and E. Harrison, Comparison of Regional Clear-Sky Albedos Inferred from Satellite Observations and Models Comparisons, *J. Clim. Appl. Meteor.*, **25**, 214-226, 1986.

Collins, W.D., P.J. Rasch, B.E. Eaton, B.V. Khattatov, J.-F. Lamarque, and C.S.

Zender, 2001: Simulating aerosols using a chemical transport model with assimilation of satellite aerosol retrievals. Methodology for INDOEX. *J. Geophs. Rev*. **106**, 7313-7336.

Dickinson, R. E., 1983:Land surface processes and climate-Surface albedos and energy balance. *Advances in Geophysics*, **25**, 305-353.

Jin, Z., T.P. Charlock, W.L. Smith, K. Rutledge, 2004: *A* Parameterization of Ocean Surface Albedo, *Geophys. Res. Ltrs.*, **31**, L.22301.

Kato, S., F.G., Rose, and T.P., Charlock, 2005: Computation of Domain-Averaged Irradiance Using Satellite-Derived Cloud Properties, *J. of Atmos. Ocean. Tech.*, **22b**, pp 146-164.

Kaufman, Y. J., D. Tanre, H. R. Gordon, T. Nakajima, J. Lenoble, R. Frouin, H. Grassl, B. M. Herman, M. D. King, and P. M. Teillet, 1997: Passive remote sensing of tropospheric aerosol and atmospheric correction for the aerosol effect. *J. Geophys. Res*., 102, 16,815-16,830.

Minnis, P.; and co-authors: Cloud Optical Property Retrieval (Subsystem 4.3). "Clouds and the Earth's Radiant Energy System (CERES) Algorithm Theoretical Basis Document, Volume III: Cloud Analyses and Radiance Inversions (Subsystem 4)", *NASA RP 1376 Vol. 3*,edited by CERES Science Team, December, 1995, pp. 135-176.

P1.1

Rose, F.G. and Charlock, T.P., 2002: New Fu-Liou code tested with ARM raman lidar aerosols and CERES in pre-CALIPSO sensitivity study. *11th Conf. on Atmos Radiation*, Ogden, UT.

Rutan, D. A., F.G. Rose, N. Smith, and T. P. Charlock, 2001: Validation data set for CERES Surface and Atmospheric Radiation Budget (SARB), WCRP GEWEX Newsletter, **11**, No. 1, 11-12.

Fu, Q., and K.N. Liou, 1993: Parameterization of the radiative properties of cirrus clouds. *J. Atmos. Sci*., **50**, 2008-2025

Wielicki, B.A., B.R. Barkstrom, E.F. Harrison, R.B. Lee, G.L. Smith, and J.E. Cooper, 1996: Clouds and the Earth's Radiant Energy System (CERES): An Earth Observing System Experiment. Bull. Amer. Meteor. Soc., 77, 853-868.